Journal of Controlled Release

Title;
Focused ultrasound/microbubbles-assisted BBB opening enhances LNP-mediated mRNA delivery to brain

Koki Ogawa[a, 1], Naoya Kato[a], Michiharu Yoshida[b], Takeshi Hiu[b], Takayuki Matsuo[b], Shusaku Mizukami[c], Daiki Omata[d], Ryo Suzuki[d, f], Kazuo Maruyama[e, f], Hidefumi Mukai[a, g], Shigeru Kawakami[a]

[a]Department of Pharmaceutical Informatics, Graduate School of Biomedical Sciences, Nagasaki University, 1-7-1 Sakamoto, Nagasaki-shi, Nagasaki, Japan
[b]Department of Neurosurgery, Nagasaki University, School of Medicine, Nagasaki University, 1-7-1 Sakamoto, Nagasaki-shi, Nagasaki, Japan
[c]Department of Immune Regulation, Shionogi Global Infectious Diseases Division, Institute of Tropical Medicine, Nagasaki University, 1-12-4 Sakamoto, Nagasaki-shi, Nagasaki, Japan
[d]Laboratory of Drug and Gene Delivery Research, Faculty of Pharma-Science, Teikyo University, 2-11-1 Kaga Itabashi-ku Tokyo, Japan
[e]Laboratory of Theranostics, Faculty of Pharma-Science, Teikyo University, 2-11-1 Kaga Itabashi-ku Tokyo, Japan
[f]Advanced Comprehensive Research Organization (ACRO), Teikyo University, 2-11-1 Kaga Itabashi-ku Tokyo, Japan
[g]Laboratory for Molecular Delivery and Imaging Technology, RIKEN Center for Biosystems Dynamics Research, 6-7-3 Minatojima-minamimachi, Chuo-ku, Kobe, Hyogo, Japan
[1] Present affiliation: Graduate School of Pharmaceutical Sciences, Department of Drug Delivery and Nano Pharmaceutics, Nagoya City University, 3-1, Tanabe-dori, Mizuho-ku, Nagoya, Japan

Abbreviations: BBB, blood-brain barrier; LNP, lipid nanoparticle; mRNA, messenger RNA; FUS, focused ultrasound

For correspondence: Shigeru Kawakami, Department of Pharmaceutical Informatics, Graduate School of Biomedical Sciences, Nagasaki University, 1-7-1 Sakamoto, Nagasaki-shi, Nagasaki 852-8588, Japan
Tel: +81-95-819-8563; Fax: +81-95-819-8563; E-mail: skawakam@nagasaki-u.ac.jp

Abstract

Messenger RNA (mRNA) medicine has become a new therapeutic approach owing to the progress in mRNA delivery technology, especially with lipid nanoparticles (LNP). However, mRNA encapsulated-LNP (mRNA-LNP) cannot spontaneously cross the blood-brain barrier (BBB) which prevents the expression of foreign proteins in the brain. Microbubble-assisted focused ultrasound (FUS) BBB opening is an emerging technology that can transiently enhance BBB permeability. In this study, FUS/microbubble-assisted BBB opening was investigated for the intravenous delivery of mRNA-LNP to the brain. The intensity of FUS irradiation was optimized to 1.5 kW/cm^2, at which BBB opening occurred efficiently without hemorrhage or edema. Exogenous protein (luciferase) expression by mRNA-LNP, specifically at the FUS-irradiated side of the brain, occurred only when FUS and microbubbles were applied. This exogenous protein expression was faster but shorter than that of plasmid DNA delivery. Furthermore, foreign protein expression was observed in the microglia, along with CD31-positive endothelial cells, whereas no expression was observed in astrocytes or neurons. These results support the addition of mRNA-LNP to the lineup of nanoparticles delivered by BBB opening.

Keywords: Blood-brain barrier (BBB), Focused ultrasound (FUS), Lipid nanoparticles (LNP), Microbubble, messenger RNA (mRNA)

Introduction

Use of messenger RNA (mRNA) medicine has become a new therapeutic approach because of the following advantages over gene therapy[1]: Therapeutic protein expression by mRNA is achieved by cytosolic delivery without concern of genome integration. Thus, mRNA medicine is expected to offer therapeutic protein with high efficiency and safety. To date, naked mRNA coding vascular endothelial growth factor A (VEGF-A) has been clinically applied for the treatment of heart failure [2] or diabetes-induced skin ischemia [3] by local injection into lesion sites. However, systemic delivery of naked mRNA is difficult; with its large size and negative charge, it cannot penetrate cell membranes and is easily decayed in blood circulation.

Nanocarriers such as polyplexes[4], lipoplexes [5], micelles [6, 7], and emulsions [8], have been intensively developed for mRNA delivery to target sites/cells. Among them, lipid nanoparticle (LNP) has achieved great success [9, 10] in protecting mRNA from degradation by encapsulating it with lipids and delivering it to target cells. Ionizable lipids, a component of LNP, play a crucial role in endosomal escape and mRNA release into the cytosol. Many studies have focused on liver targeting because typical LNP are taken up by hepatocytes [11]. Recently, LNP with tropism toward extrahepatic organs (e.g., tumor [12], lung [13]) have been developed by incorporating functionalized lipids or modifying targeting moieties on the surface of LNP. In the case of brain-targeted LNP, the blood-brain barrier (BBB) is a major obstacle; therefore, its demonstration has been very limited to LNP modified with neurotransmitters as brain-targeting ligands [14]. In addition, this type of brain-targeted LNP deliver mRNA to a wide area of the brain, which can raise concerns about unexpected adverse effects. Thus, technologies to transport these drugs to the brain's more restricted areas need to be developed.

Microbubble-assisted focused ultrasound (FUS)-induced BBB opening is an emerging technique for low-invasive drug delivery to the brain [15, 16]. When FUS is irradiated to the target location of the brain following intravenous (IV) injection of ultrasound-responsible microbubbles, oscillation or cavitation energy is produced in the blood vessels of the irradiated site, which induces transient BBB opening [15]. Because BBB opening is induced in a restricted manner at the irradiated area of the brain, drugs can be delivered selectively to the intended region. FUS/microbubble -assisted BBB opening has been demonstrated even in patients with amyotrophic lateral sclerosis and Alzheimer's disease by magnetic resonance imaging (MRI), in which extravasation of MRI contrast agent was confirmed [17, 18]. For the application of ultrasound-mediated drug delivery to the brain, we and other researchers have successfully delivered anticancer drugs [19, 20] or plasmid DNA in preclinical studies [21-24]. Moreover, our group achieved BBB opening using our recently developed more stable microbubbles with higher content of echogenic gas [25]. However, to the best of our knowledge, there have been no reports on the delivery of mRNA-LNP using microbubble-assisted FUS-induced BBB opening.

In this study, we delivered mRNA-LNP to the brain of mice using microbubble-assisted FUS-

induced BBB opening. Characteristics of foreign protein expression in the brain were evaluated using mRNA-coding reporter gene (firefly luciferase or ZsGreen1). In particular, we identified cells expressing ZsGreen1 in the brain using immunohistological examination.

Materials and methods

Synthesis of in vitro transcription (IVT) mRNA

Plasmid DNA carrying firefly luciferase and subsequent 120-bp poly (A/T) sequence was constructed by custom artificial gene synthesis. Plasmid DNA carrying ZsGreen1 was constructed by inserting the ZsGreen1 cDNA fragment from pZsGreen1-N1 vector (Clontech, Palo Alto, CA, USA) into upstream of poly(A/T) sequence. Each plasmid DNA was amplified in DH5α *Escherichia coli* strain and purified using NucleoSpin Plasmid Transfection-grade (MACHEREY-NAGEL GmbH & Co. KG, Germany). Plasmid DNA was linearized at the end of poly (A/T) sequence using SapI restriction enzyme. Linearized DNA was then subjected to IVT, performed using HiScribe T7 High Yield RNA Synthesis Kit (New England Biolabs Japan Inc.) combined with CleanCap® Reagent AG (TriLink BioTechnologies) as per the instruction manual.

Preparation of mRNA encapsulated LNP

mRNA-LNP were prepared by mixing lipids and mRNAs in a microfluidic system with reference to the literature [26]. Briefly, COATSOME SS-OP (NOF, Tokyo, Japan), DOPC (NOF), cholesterol (Nacalai Tesque Inc., Kyoto, Japan), and DMG-PEG2000 (NOF) were dissolved in ethanol. The molar ratio of each lipid was 60/10/30, and DMG-PEG2000 was added at 1.5 mol% of the total lipid. mRNA was diluted in 20 mM malic acid buffer (pH 3.0). Lipid (4.5 mM) and mRNA solutions (7.5 μg/mL) were mixed using NanoAssemblr® Benchtop (Precision NanoSystems, Inc.) under the following conditions: total flow rate of 4 mL/min and flow rate ratio of 3:1 (mRNA:lipid). The resultant solution was dialyzed against 20 mM MES buffer (pH 6.5) to remove ethanol and then concentrated using ultrafiltration. Finally, LNP were suspended in phosphate-buffered saline (PBS).

Characteristics of LNP

The size and zeta potential of LNP were measured using Zetasizer Nano ZS (Malvern Instruments, Malvern, UK). Diluted LNP were introduced into capillary cells and measured at 25˚C.

To measure the encapsulation efficiency of mRNA-LNP, Quant-iT™ RiboGreen™ RNA Assay Kit (Thermo) was used to quantify mRNA. Unencapsulated mRNA concentration was measured by quantifying intact mRNA-LNP, while the total mRNA concentration was measured by solubilization with a final concentration of 0.4% Triton X-100. Encapsulation efficiency was calculated using the following formula:

$$\text{Encapsulation efficiency } (\%) = \frac{(\text{total mRNA}) - (\text{unencapsulated mRNA})}{\text{total mRNA}} \times 100$$

Preparation of microbubbles

Microbubbles composed of DSPC, DSPG, and DSPE-PEG2000 were prepared as previously reported [25]. Briefly, liposomes composed of DSPC, DSPG, and DSPE-PEG2000 at a molar ratio of 30:60:10 were prepared using the hydration method. Liposomes (1 mM lipid in 100 mM phosphate buffer, pH 7.4) were homogenized with perfluoropropane (Takachiho Chemical Industrial Co., Ltd., Tokyo, Japan) using Labolution Mark II mixer (PRIMIX Corporation, Hyogo, Japan) at 7,500 rpm at 40°C for 1 h. The microbubble dispersion was mixed with 18% sucrose in a 1:1 (v/v) ratio. The mixture was transferred to a vial and freeze-dried (Eyela FDU-1100 freeze-dryer and DRU-1100 sample chamber; Tokyo Rikakikai Co., Ltd., Tokyo, Japan). The headspace of the vial was filled with perfluoropropane, and the vial was closed with a rubber lid and an aluminum cap. The freeze-dried microbubbles were rehydrated with MilliQ water and filtered using a mini-spike filter (B. Braun Aesculap Japan Co. Ltd., Tokyo, Japan) before use. The number and size of the microbubbles were measured using Coulter counter (Multisizer 3; Beckman Coulter, Tokyo, Japan).

Animal

Five-week-old male ddY mice (25–30 g) were purchased from Japan SLC, Inc. (Hamamatsu, Japan), housed in cages in an air-conditioned room, and maintained on a standard laboratory diet (MF; Oriental Yeast Co., Ltd., Tokyo, Japan), with food and water available *ad libitum*. Before treatment, the mice were anesthetized with three types of mixed anesthetic agents. All animal experiments were performed in accordance with the guidelines for animal experimentation of Nagasaki University and were approved by the Institutional Animal Care and Use Committee of Nagasaki University (approval number: 1308051086-6).

FUS irradiation to mice brain

The FUS irradiation and mouse-fixing device are shown in Fig. 1a. FUS was used to irradiate mouse brains using Sonitron 5000 HIFU (Nepa Gene Co. Ltd., Chiba, Japan) connected to a cylindrical transducer, which was filled with 1% agarose gel. Ultrasonic gel was placed on the agarose to fill the gap. After the mice were anesthetized, the scalp fur was removed. The head was placed on ultrasonic gel, and then the position was adjusted using a laser marking device to irradiate the targeted region of the brain. FUS was irradiated to the right striatum at following conditions: frequency, 3 MHz; intensity, 0.5–1.5 kW/cm^2; duration, 60 sec; duty cycle, 10% (1 msec irradiation and 9 msec interval).

Evans blue extravasation

BBB opening was confirmed using Evans blue extravasation. Evans blue at 100 mg/kg and

microbubbles (5×10^9 particles/kg) were administered to mice intravenously, and FUS was irradiated as described above. Two hours post irradiation, the brains were removed after perfusion with PBS. The brains were dissected at 2 mm interval, and the striatum, where FUS was irradiated, was observed.

Delivery of mRNA encapsulated LNP to brain

mRNA-LNP at 1.25, 2.5, or 5 μg (in terms of mRNA) and microbubbles (5×10^9 particles/kg), were administered intravenously at 1 min apart. Mice were then placed on the FUS apparatus 1 min after microbubble administration, and the FUS was irradiated as described above.

Luciferase assay

Luciferase expression levels in the brain were measured several times after delivery of luciferase mRNA-encapsulated LNP. Mouse brains were divided into right (irradiated side) and left (un-irradiated side) hemispheres (Fig. 2b). Each brain sample was homogenized in lysis buffer (0.1 M Tris, 2.5 mM EDTA, 0.05% Triton X-100, pH 7.8). The homogenate was reacted with PicaGene luciferase substrate (Toyobo, Osaka, Japan). Luciferase expression level was standardized by total protein; the result is presented as "pg luciferase/mg protein."

Immunohistochemistry

After delivery of ZsGreen1 mRNA-encapsulated LNP, ZsGreen1 distribution in the brain of the FUS-irradiated site was evaluated by immunohistochemistry. Twelve hours after the administration of mRNA-LNP, the mice were perfused with PBS followed by 4% paraformaldehyde (PFA) solution for fixation. Brain samples were collected and further fixated by immersing in PFA solution. Cryoprotection was performed by immersion in 20% and 30% sucrose solutions before the samples were frozen in optimal cutting temperate compound at -80°C. A 50-μm-thick tissue section was prepared using a cryostat. After the brain sections were mounted onto the glass slides, 5% normal goat serum was added for blocking. To stain endothelial cells with CD31, anti-mouse CD31 (MEC13.3, BioLegend) (1:100) and Alexa Fluor 647 conjugated anti-rat IgG (polyclonal, Jackson ImmunoResearch) (1:200) were used. Astrocytes, neurons, and microglia were co-stained with CD31. Anti-GFAP (polyclonal, Proteintech) (1:500), Alexa Fluor 594 conjugated anti-MAP2 (SMI 52, BioLegend), and anti-Iba1 (NCNP24, FUJIFILM Wako) (1:500) were mixed with anti-mouse CD31 (1:100). The appropriate secondary antibodies were then added.

Confocal laser microscopy

After staining, cover glasses were mounted onto the glass slides with mounting medium (SlowFade™ Glass, Thermo). Samples were analyzed using a confocal laser microscope (LSM 800, Carl Zeiss Microimaging GmbH, Jena, Germany) equipped with 40× oil immersion objective lens. Z-

stack images (interval; 0.4 μm) were acquired.

Statistical analysis

Statistical comparisons were performed by two-way ANOVA followed by Bonferroni's multiple comparisons test using GraphPad Prism software. Statistical significance was set at $p < 0.05$.

Results

Characterization of microbubbles

The number and size of microbubbles were evaluated using Coulter counter. Number of microbubbles was 1.1×10^9 particles/mL and the average size, based on the volume distribution of the microbubbles, was 2.6 μm.

Evaluation of BBB opening induced by FUS/microbubbles using Evans blue extravasation

By placing the heads of anesthetized mice on the silicon fixation platform (Fig. 1a), FUS was reproducibly irradiated to the targeted area (right striatum). Fig. 1b shows the whole brains at 2-mm thick coronal slices removed from Evans blue-pretreated mice, euthanized after 2 h of FUS/microbubble treatment. Evans blue extravasation was observed selectively in and around the right striatum, the center of FUS irradiation, and the degree of extravasation increased with increasing irradiation intensity. In particular, since no hemorrhage or edema was observed in the brains despite high Evans blue extravasation at 1.5 kW/cm^2, subsequent experiments were conducted at this intensity.

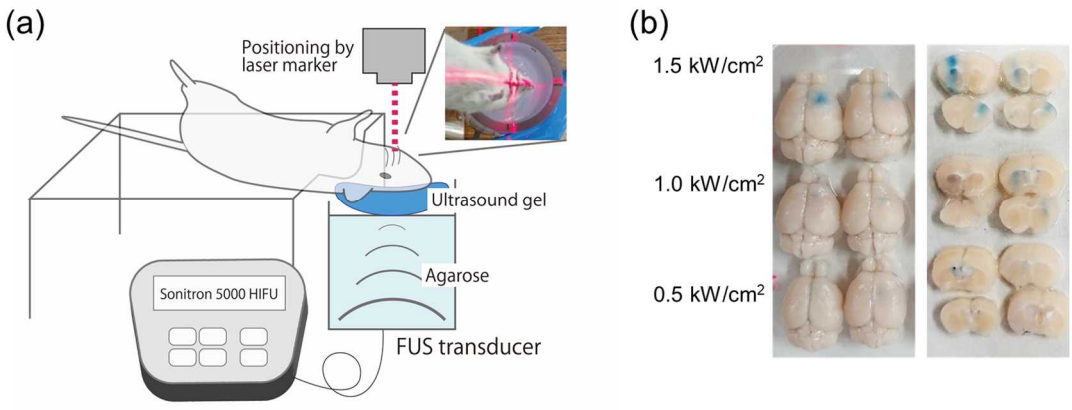

Fig. 1. FUS and microbubbles-mediated BBB opening system.

(a) FUS irradiation apparatus used in this study. Cylindrical FUS transducer was filled with 1% agarose gel and ultrasound gel. Mice body were placed on the custom-built fixed base, and the head was horizontally placed on ultrasonic gel. Head position was adjusted using a laser marking device to irradiate the targeted region of the brain. Then, FUS was irradiated to the right striatum.

(b) Evans blue extravasation induced by microbubbles injection followed by the FUS irradiation at various intensity.

Characteristics of mRNA-LNP

mRNA-LNP with high uniformity were reproducibly fabricated. The data of dynamic light scattering and electrophoretic light scattering of luciferase-mRNA-LNP in PBS show that the particle sizes (Z-average) were 93.1 ± 4.5 nm with the PDI of 0.12 ± 0.08 and zeta potential values were -3.64 ± 0.98 mV. The encapsulation efficiency of mRNA was 97.9 ± 0.50%. Values represent mean ± SD (n=3). The physicochemical properties and encapsulation efficiency of the mRNA-LNP encoding ZsGreen1 were similar.

Enhancement of LNP-mediated mRNA delivery to the brain via FUS/microbubble-induced BBB opening

Luciferase expression levels were approximately 0.3–0.4 pg/mg protein in both right and left hemispheres of brains at 6 h after administration of luciferase mRNA-LNP (Fig 2a). After luciferase mRNA-LNP administration, neither additional FUS irradiation nor microbubble administration changed the luciferase expression levels in either the right or left hemisphere. In contrast, when luciferase mRNA-LNP were administered with both FUS irradiation and microbubbles, the luciferase expression levels increased to 7.1 pg/mg protein on the right side of the brain, including the right striatum, where FUS irradiation was located, and the difference was statistically significant. No such increase was observed in the left side of the brain.

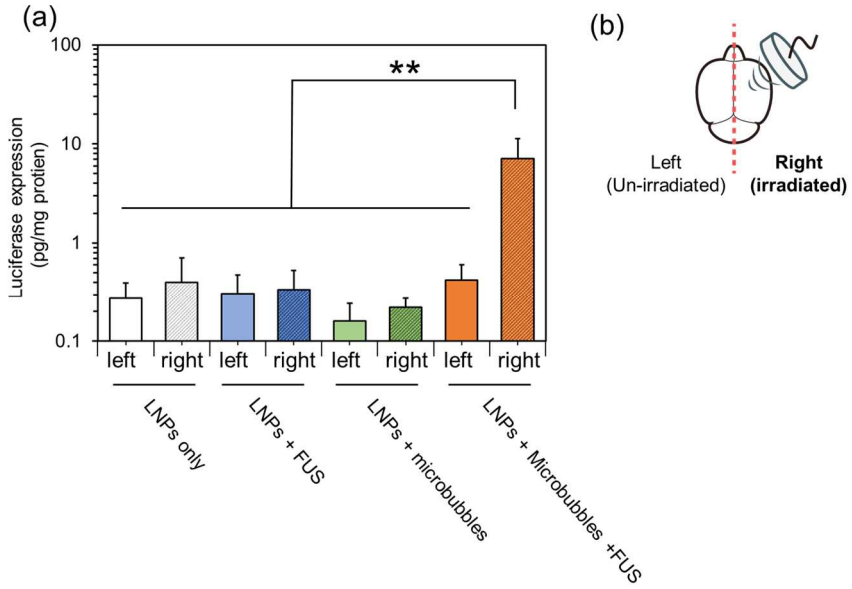

Fig. 2. Luciferase protein expression in the brain induced by FUS and microbubbles-mediated BBB opening.
Mice were administered with luciferase mRNA-LNP (2.5 μg) followed by microbubbles injection and FUS irradiation to right hemisphere of the brain. Six hours after the delivery of mRNA-LNP, the brain was divided into left and right hemispheres as shown in (b) and luciferase expression level was evaluated. (a) Luciferase expression level obtained by the mRNA-LNP. Data represent mean ± SD (n=3). Statistical significance was calculated with two-way ANOVA with Bonferroni's test. ** $p < 0.01$.

Effect of mRNA-LNP dose on protein expression levels in the brain

When the dose of luciferase mRNA-LNP was increased from 1.25 to 5 μg/mouse along with microbubble administration (without FUS irradiation), luciferase expression levels in the right hemisphere increased in a dose-dependent manner from 0.14 to 2.4 pg/mg protein (Fig. 3). In contrast, when microbubbles-assisted FUS-induced BBB opening was performed targeting the right striatum, the luciferase expression levels in the right brain were 6.0 pg/mg protein even at a dose of 1.25 μg/mouse. When the dose was increased to 5 μg/mouse, the levels did not change.

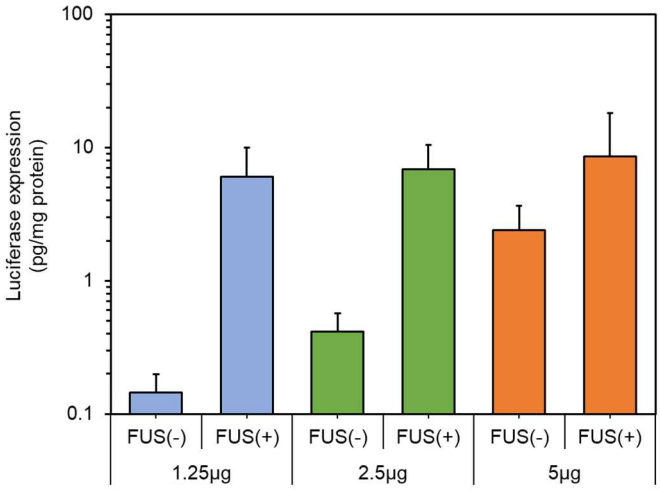

Fig. 3. Effect of mRNA dose on exogenous protein expression in the brain.
Luciferase expression levels obtained by the administration of various doses of LNP (1.25, 2.5, 5 μg) followed by microbubbles injection with or without FUS irradiation to right hemisphere of brain. Six hours after the delivery of mRNA-LNP, the brain was divided into right and left hemispheres and luciferase expression levels of right hemisphere were evaluated. Data represent mean ± SD (n=3). There were no significant differences analyzed by two-way ANOVA with Bonferroni's test.

Distribution of foreign protein expression in the brain

Three-dimensional images of 50-μm-thick brain sections removed from mice, euthanized 12 h after the administration of mRNA-LNP encoding ZsGreen1, were immunologically counterstained with CD31 (Fig. 4). Widespread distribution of ZsGreen1 expression was observed at the FUS-irradiated sites and was mostly colocalized with CD31-positive endothelial cells (Fig. 4a). In addition, part of ZsGreen1 was present outside the vascular structures visualized by CD31-positive endothelial cells (Fig. 4b). Further, ZsGreen1 signals outside the blood vessels partially overlapped with those of Iba1-positive microglia (Fig. 5c, f). In contrast, no overlap with the GFAP-positive astrocytes or MAP2-positive neurons were noted (Fig. 5a, b, d, e).

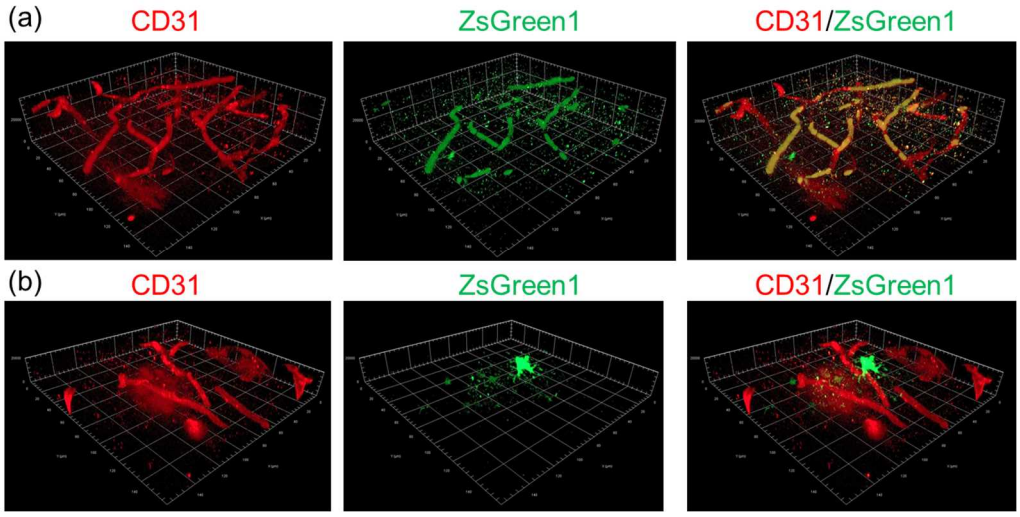

Fig. 4. Distribution analysis of exogenous protein expression induced by mRNA-LNP and BBB opening

Twelve hours after the delivery of ZsGreen1 mRNA-LNP by FUS-mediated BBB opening, brain sections were immunologically stained with CD31. FUS irradiated region was observed. (a) ZsGreen1 expression on CD31-expressing endothelial cells. (b) ZsGreen1 expression outside endothelial cells. Red (left column) and green (meddle column) shows the signal of CD31 and ZsGreen1, respectively. Right column shows merged image.

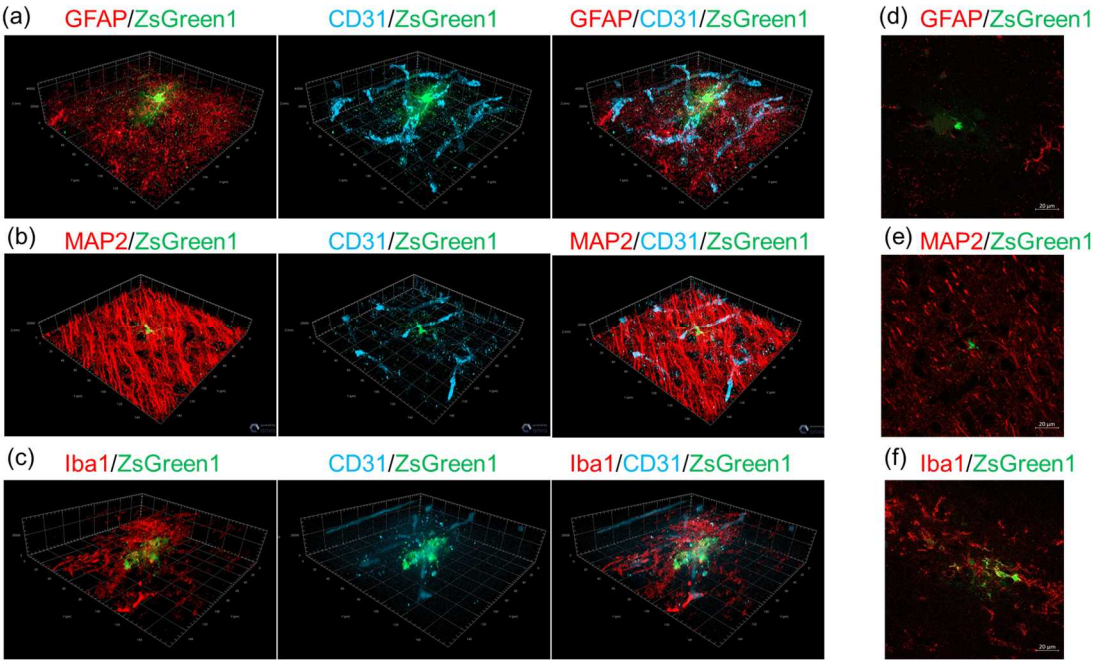

Fig. 5. Identification of protein expressing cells induced by mRNA-LNP and BBB opening
Twelve hours after the delivery of ZsGreen1 mRNA-LNP by FUS-mediated BBB opening, brain samples were immunologically stained with CD31 combined with GFAP (a,d), MAP2 (b,e), or Iba1 (c,f). FUS irradiated region was observed. Red signals in (a), (b), and (c) indicate GFAP, MAP2, and Iba1, respectively. Cyan signals observed in (a), (b), and (c) indicate CD31. Green signals indicate ZsGreen1. (a,b,c) Z-stack image. (d,e,f,) 2D image of interested region.

Time-course profiles of foreign protein expression in the brain

At 3 h after luciferase mRNA-LNP administration with the dose of 2.5 μg mRNA, luciferase expression level in the right hemisphere, the FUS-irradiated side of the brain, was 8.4 pg/mg protein, and this level was sustained until 12 h after administration, with a tendency to slightly decrease to 1.2 pg/mg protein at 24 h after administration.

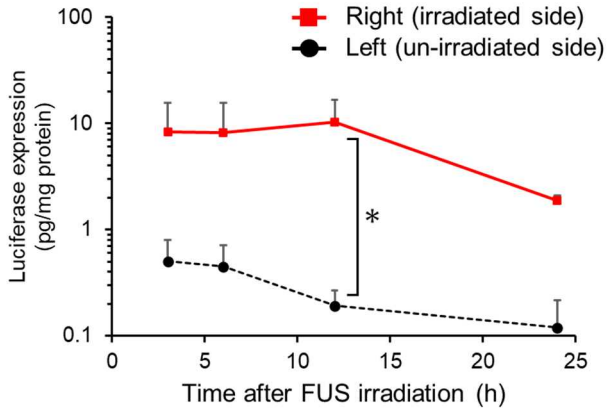

Fig. 6. Time-course profile of exogenous protein expression in the brain.
Time-course luciferase expression level obtained by the administration of mRNA-LNP (2.5 μg) followed by microbubbles injection and FUS irradiation to right hemisphere of brain. After 3, 6, 12, 24 h of the treatment, the brain was divided into right and left hemispheres and luciferase expression levels were measured. Data represent mean ± SD (n=4). Statistical significance was calculated with two-way ANOVA with Bonferroni's test. * $p < 0.05$.

Discussion

In this study, we demonstrated that FUS/microbubble -assisted BBB opening enhanced LNP-mediated mRNA delivery to the brain without any hemorrhage or edema in mice. The mRNA-LNP crossed the BBB, and foreign proteins were found to be expressed in microglia along with endothelial cells.

Previous animal studies demonstrated the basic effects and safety of using planar ultrasound in BBB opening [25]. However, the results obtained in this study, showing that the extravasation of Evans blue dye localized to the irradiated striatum without apparent bleeding or edema by using FUS (Fig. 1b), indicate the validity of replacing planar ultrasound with FUS in future studies of BBB

opening. There is already a clinical device that irradiates FUS under MRI guidance. Although there are only a few clinical studies that achieved BBB opening with microbubble-assisted FUS, no serious adverse events were observed in patients [17, 18]. Thus, the safety of FUS/microbubble -assisted BBB opening, which is the biggest barrier to the clinical application of this mRNA delivery method, has been verified. Although a more detailed study is needed, this information will support a smooth translation in the future. The optimized FUS intensity in this study was 1.5 kW/cm^2, because excessive FUS irradiation can cause hemorrhage [27, 28].

The physicochemical properties of the mRNA-LNP used in this study (approximately 100 nm in size, monodisperse, and neutral surface charge) and almost 100% encapsulation efficiency were in alignment with those of mRNA-LNP containing ionizable lipids, including SS-OP [26]. Exogenous protein (luciferase) expression by mRNA-LNP, specifically at the FUS-irradiated side of the brain, occurred only when FUS and microbubbles were applied to open the BBB (Fig. 2a). This is consistent with our previous result of BBB opening-assisted plasmid DNA delivery to the brain by planar ultrasound irradiation post administration of bubble lipopolyplexes with adjusted surface charge [22]. In contrast, the time-course profile of exogenous protein expression, which was already at the same level as the peak at 3 h post administration and started to decline at 24 h (Fig. 6), indicated that the protein expression by this method starts and decreases early compared to the gene delivery using plasmid DNA. This is consistent with the characteristics of foreign protein expression using mRNA, which does not require a nuclear transfer process unlike gene delivery using plasmid DNA. When considering mRNA therapy for neurological diseases, concerns about short protein expression periods may be resolved by multiple doses. For example, Fukushima et al.(2021) successfully treated ischemic stroke with multiple intracerebroventricular (ICV) injections of nanomicelles, including brain-derived neurotrophic factor-mRNA [7]. Considering the burden to patients, an approach combining minimally invasive systemic administration and external stimulation with a medical device may be more suitable for multiple doses than local administration. Thus, BBB opening-mediated mRNA-LNP delivery can be a suitable DDS approach for mRNA-based neurological disease therapies.

Under similar conditions of BBB opening without intracerebral bleeding as in this study, BBB permeability after BBB opening is reported to decrease in 50% within 3 h [29]. In addition, typical LNPs for mRNA delivery, equivalent to the LNP used in this study, are quickly eliminated from the blood circulation and accumulated in liver within 0.5-1 h [30]. Thus, BBB opening duration obtained in this study may be enough to translocate mRNA-LNP to brain. Some studies have shown that BBB opening duration is controllable by adjusting some parameters especially FUS intensity [29] and microbubble character [31]. Therefore, therapeutic application of this approach is expected by further optimization of minimal BBB opening for translocation of mRNA-LNP to brain.

Interestingly, while dose dependency of foreign protein expression was linear in mRNA-LNP delivery without functional BBB opening (without FUS), it was nonlinear and did not change

with increasing dose in the BBB opening-assisted approach (Fig. 3). This result implies that a lower mRNA-LNP dosage is sufficient for the BBB opening-assisted approach, whereas an increase in protein expression by increasing the dosage is not expected. The fundamental mechanism of BBB permeabilization is thought to be the formation of a BBB opening gap and subsequent downregulation of BBB components (claudin, occludin, and ZO-1) [23]. Considering that the BBB penetration efficiency of nanoparticles induced by BBB opening depends on the size of nanoparticles, and that the efficiency of nanoparticles with a diameter of approximately 120-nm diameter was drastically lower than that of nanoparticles with 15-nm diameter [32]. Recently, FUS/microbubble was reported to promote endocytosis and transcytosis and attribute to the uptake and penetration of large molecule in/across brain endothelial cells [33, 34]. Based on the non-linear luciferase expression in the brain in FUS(+) group (Fig. 5), the endocytosis and transcytosis, which are energy-dependent, can be one of the key mechanisms, although further investigation is necessary.

When the dose of mRNA-LNP increased, luciferase expression level in the brain of FUS(-) group became close to that of FUS(+) group at a mRNA dose of 5 μg (Fig. 3). It was showed that lipid-based nanocarriers (without special brain-targeting ligands) did not penetrate BBB in a normal mice [35, 36]; therefore, they could not cause protein expression in brain parenchyma even when the dose of LNP is increased. Thus, it is strongly suggested that the dose-dependent increase in the luciferase expression in FUS(-) group was caused by the increased expression in endothelial cells of brain. On the other hand, distribution analysis revealed that BBB opening made protein expression in the brain parenchyma especially microglia (Fig. 5), although the amount was relatively small compared with protein expression in endothelial cells. Even if the luciferase expression in the whole brain was equivalent, its distribution of protein expression by mRNA was thought to be changed by the FUS irradiation.

In the immunohistological analysis combined with ZsGreen1 mRNA-LNP administration, foreign protein expression was observed in microglia along with CD31-positive endothelial cells, while no expression was found in astrocytes or neurons (Fig. 4 and 5). The uptake mechanism of typical LNP consisting of ionizable lipids is as follows: LNP are coated with apolipoprotein E (ApoE) in blood circulation [37], and then ApoE-coated LNP undergo endocytosis into cells via ApoE receptor (such as low-density lipoprotein receptor [LDLR]) [38]. Microglia express LDLR [39], may be associated with preferential foreign protein expression in microglia compared with astrocytes and neurons. In contrast, a study on ICV administration of mRNA-LNP concluded that exogenous proteins were expressed in neurons and astrocytes [40]. This conflicting result is possibly due to the physiological reaction caused by FUS/microbubble-assisted BBB opening, along with the differences in the accessibility of mRNA-LNP to each cell type due to the different routes of administration. It has been reported that FUS/microbubble-assisted BBB opening induces microglial activation, along with sterile inflammation, even without hemorrhage [41]. Microglia seem to take in macromolecules in the

activated state more effectively than in the normal state, which may lead to ZsGreen1 expression in microglia.

The limitation of our distribution analysis is the lack of quantitative and comprehensive information because tissue section-based evaluation can obtain information at a restricted region of interest. Methods utilizing tissue-clearing techniques have been developed for more comprehensive observation of foreign protein expression in three-dimensional tissues [21, 42-44]. However, it is still difficult to combine these with an immunohistochemical approach with high flexibility; therefore, in this study, we used tissue sections for examination. Further improvement on tissue clearing technology will enable more accurate evaluation of protein expression distribution in the brain after mRNA-LNP delivery with FUS/microbubble-assisted BBB opening in the future.

mRNA medicine is a promising approach for the treatment of neurological diseases. Several carriers have been reported to deliver mRNA to the brain, including micelles [7], polyplexes [4], and LNP [40]. However, these delivery systems have been limited to local administration, such as ICV or intracranial injection, along with highly invasive procedures. Therefore, a minimally invasive delivery approach using a systemic route is required. While typical LNP are thought to be potent mRNA carriers, especially for liver-targeting or vaccine applications, these cannot penetrate the BBB nor induce protein expression in the brain parenchyma. We and other groups have reported that FUS/microbubble-assisted BBB opening can deliver a variety of nanocarriers to the brain via IV administration [22, 24, 32, 45]. This study adds mRNA-LNP to the lineup of nanoparticles delivered by BBB opening.

Conclusion

In this study, we demonstrated for the first time that mRNA-LNP induce foreign protein expression across the BBB via systemic route using FUS-mediated BBB opening. Microbubble injection and FUS irradiation selectively increased BBB permeability in the irradiated region, which enhanced exogenous protein expression induced by mRNA-LNP. Partial exogenous proteins were produced in the brain parenchyma outside blood vessels. Moreover, we revealed that microglia may undergo protein expression via mRNA-LNP delivery system, although detailed analysis to clarify the transfer mechanism is desired. We believe that the brain-targeted mRNA delivery system developed in this study provides a minimally invasive platform for mRNA-based medicine for neurological disorders.

Acknowledgements

This work was partly supported by JSPS KAKENHI Grant Number 21H03818 (S.K.) and AMED Grant Number JP21ak0101178.

Reference

1. U. Sahin, K. Kariko, and O. Tureci, mRNA-based therapeutics--developing a new class of drugs. *Nat Rev Drug Discov*, 2014. **13**(10): 759-80.
2. V. Anttila, A. Saraste, J. Knuuti, et al., Synthetic mRNA Encoding VEGF-A in Patients Undergoing Coronary Artery Bypass Grafting: Design of a Phase 2a Clinical Trial. *Mol Ther Methods Clin Dev*, 2020. **18**: 464-472.
3. L.M. Gan, M. Lagerstrom-Fermer, L.G. Carlsson, et al., Intradermal delivery of modified mRNA encoding VEGF-A in patients with type 2 diabetes. *Nat Commun*, 2019. **10**(1): 871.
4. J. Oh, S.M. Kim, E.H. Lee, et al., Messenger RNA/polymeric carrier nanoparticles for delivery of heme oxygenase-1 gene in the post-ischemic brain. *Biomater Sci*, 2020. **8**(11): 3063-3071.
5. L.M. Kranz, M. Diken, H. Haas, et al., Systemic RNA delivery to dendritic cells exploits antiviral defence for cancer immunotherapy. *Nature*, 2016. **534**(7607): 396-401.
6. N. Oyama, M. Kawaguchi, K. Itaka, et al., Efficient Messenger RNA Delivery to the Kidney Using Renal Pelvis Injection in Mice. *Pharmaceutics*, 2021. **13**(11).
7. Y. Fukushima, S. Uchida, H. Imai, et al., Treatment of ischemic neuronal death by introducing brain-derived neurotrophic factor mRNA using polyplex nanomicelle. *Biomaterials*, 2021. **270**: 120681.
8. L.A. Brito, M. Chan, C.A. Shaw, et al., A cationic nanoemulsion for the delivery of next-generation RNA vaccines. *Mol Ther*, 2014. **22**(12): 2118-2129.
9. H. Mukai, K. Ogawa, N. Kato, et al., Recent advances in lipid nanoparticles for delivery of nucleic acid, mRNA, and gene editing-based therapeutics. *Drug Metab. Pharmacokinet.*, 2022. **44**: 100450.
10. M.D. Buschmann, M.J. Carrasco, S. Alishetty, et al., Nanomaterial Delivery Systems for mRNA Vaccines. *Vaccines*, 2021. **9**(1).
11. D. Witzigmann, J.A. Kulkarni, J. Leung, et al., Lipid nanoparticle technology for therapeutic gene regulation in the liver. *Adv Drug Deliv Rev*, 2020. **159**: 344-363.
12. Y. Sakurai, W. Mizumura, K. Ito, et al., Improved stability of siRNA-loaded lipid nanoparticles prepared with a PEG-monoacyl fatty acid facilitates ligand-mediated siRNA delivery. *Mol Pharm*, 2020. **17**(4): 1397-1404.
13. H. Parhiz, V.V. Shuvaev, N. Pardi, et al., PECAM-1 directed re-targeting of exogenous mRNA providing two orders of magnitude enhancement of vascular delivery and expression in lungs independent of apolipoprotein E-mediated uptake. *J Control Release*, 2018. **291**: 106-115.
14. F. Ma, L. Yang, Z. Sun, et al., Neurotransmitter-derived lipidoids (NT-lipidoids) for enhanced brain delivery through intravenous injection. *Sci. Adv.*, 2020. **6**(30): eabb4429.
15. M. Aryal, C.D. Arvanitis, P.M. Alexander, et al., Ultrasound-mediated blood-brain barrier disruption for targeted drug delivery in the central nervous system. *Adv Drug Deliv Rev*, 2014. **72**:

94-109.

16. K. Ogawa, N. Kato, and S. Kawakami, Recent Strategies for Targeted Brain Drug Delivery. *Chem. Pharm. Bull*, 2020. **68**(7): 567-582.
17. A. Abrahao, Y. Meng, M. Llinas, et al., First-in-human trial of blood-brain barrier opening in amyotrophic lateral sclerosis using MR-guided focused ultrasound. *Nat Commun*, 2019. **10**(1): 4373.
18. N. Lipsman, Y. Meng, A.J. Bethune, et al., Blood-brain barrier opening in Alzheimer's disease using MR-guided focused ultrasound. *Nat Commun*, 2018. **9**(1): 2336.
19. Y. Miura, Y. Fuchigami, M. Hagimori, et al., Evaluation of the targeted delivery of 5-fluorouracil and ascorbic acid into the brain with ultrasound-responsive nanobubbles. *J Drug Target*, 2018. **26**(8): 684-691.
20. X. Wang, P. Liu, W. Yang, et al., Microbubbles coupled to methotrexate-loaded liposomes for ultrasound-mediated delivery of methotrexate across the blood-brain barrier. *Int J Nanomedicine*, 2014. **9**: 4899-909.
21. K. Ogawa, Y. Fuchigami, M. Hagimori, et al., Ultrasound-responsive nanobubble-mediated gene transfection in the cerebroventricular region by intracerebroventricular administration in mice. *Eur J Pharm Biopharm*, 2019. **137**: 1-8.
22. K. Ogawa, Y. Fuchigami, M. Hagimori, et al., Efficient gene transfection to the brain with ultrasound irradiation in mice using stabilized bubble lipopolyplexes prepared by the surface charge regulation method. *Int J Nanomedicine*, 2018. **13**: 2309-2320.
23. X. Shang, P. Wang, Y. Liu, et al., Mechanism of low-frequency ultrasound in opening blood-tumor barrier by tight junction. *J Mol Neurosci*, 2011. **43**(3): 364-9.
24. B.P. Mead, P. Mastorakos, J.S. Suk, et al., Targeted gene transfer to the brain via the delivery of brain-penetrating DNA nanoparticles with focused ultrasound. *J Control Release*, 2016. **223**: 109-117.
25. D. Omata, T. Maruyama, J. Unga, et al., Effects of encapsulated gas on stability of lipid-based microbubbles and ultrasound-triggered drug delivery. *J Control Release*, 2019. **311-312**: 65-73.
26. H. Tanaka, T. Takahashi, M. Konishi, et al., Self‐degradable lipid‐like materials based on "Hydrolysis accelerated by the intra‐Particle enrichment of reactant (HyPER)" for messenger RNA delivery. *Adv. Funct. Mater.*, 2020: 1910575.
27. C.H. Fan, H.L. Liu, C.Y. Ting, et al., Submicron-bubble-enhanced focused ultrasound for blood-brain barrier disruption and improved CNS drug delivery. *PLoS One*, 2014. **9**(5): e96327.
28. J. Shin, C. Kong, J.S. Cho, et al., Focused ultrasound-mediated noninvasive blood-brain barrier modulation: preclinical examination of efficacy and safety in various sonication parameters. *Neurosurg Focus*, 2018. **44**(2): E15.
29. P.C. Chu, W.Y. Chai, C.H. Tsai, et al., Focused ultrasound-induced blood-brain barrier opening:

association with mechanical index and cavitation index analyzed by dynamic contrast-enhanced magnetic-resonance imaging. *Sci Rep*, 2016. **6**: 33264.

30. B.L. Mui, Y.K. Tam, M. Jayaraman, et al., Influence of polyethylene glycol lipid desorption rates on pharmacokinetics and pharmacodynamics of siRNA lipid nanoparticles. *Mol Ther Nucleic Acids*, 2013. **2**: e139.
31. B. Marty, B. Larrat, M. Van Landeghem, et al., Dynamic study of blood-brain barrier closure after its disruption using ultrasound: a quantitative analysis. *J Cereb Blood Flow Metab*, 2012. **32**(10): 1948-58.
32. S. Ohta, E. Kikuchi, A. Ishijima, et al., Investigating the optimum size of nanoparticles for their delivery into the brain assisted by focused ultrasound-induced blood–brain barrier opening. *Sci.Rep.*, 2020. **10**(1): 18220.
33. I. De Cock, E. Zagato, K. Braeckmans, et al., Ultrasound and microbubble mediated drug delivery: acoustic pressure as determinant for uptake via membrane pores or endocytosis. *J Control Release*, 2015. **197**: 20-8.
34. R. Pandit, W.K. Koh, R.K.P. Sullivan, et al., Role for caveolin-mediated transcytosis in facilitating transport of large cargoes into the brain via ultrasound. *J Control Release*, 2020. **327**: 667-675.
35. O.A. Marcos-Contreras, C.F. Greineder, R.Y. Kiseleva, et al., Selective targeting of nanomedicine to inflamed cerebral vasculature to enhance the blood-brain barrier. *Proc Natl Acad Sci U S A*, 2020. **117**(7): 3405-3414.
36. I. Khalin, N. Adarsh, M. Schifferer, et al., Size-selective transfer of lipid nanoparticle-based drug carriers across the blood brain barrier via vascular occlusions following traumatic brain injury. *Small*, 2022: e2200302.
37. F. Sebastiani, M. Yanez Arteta, M. Lerche, et al., Apolipoprotein E binding drives structural and compositional rearrangement of mRNA-containing lipid nanoparticles. *ACS Nano*, 2021. **15**(4): 6709-6722.
38. A. Akinc, W. Querbes, S. De, et al., Targeted delivery of RNAi therapeutics with endogenous and exogenous ligand-based mechanisms. *Mol Ther*, 2010. **18**(7): 1357-64.
39. B.A. Loving and K.D. Bruce, Lipid and lipoprotein metabolism in microglia. *Front Physiol*, 2020. **11**: 393.
40. H. Tanaka, T. Nakatani, T. Furihata, et al., In vivo introduction of mRNA encapsulated in lipid nanoparticles to brain neuronal cells and astrocytes via intracerebroventricular administration. *Mol Pharm*, 2018. **15**(5): 2060-2067.
41. Z.I. Kovacs, S. Kim, N. Jikaria, et al., Disrupting the blood-brain barrier by focused ultrasound induces sterile inflammation. *Proc Natl Acad Sci U S A*, 2017. **114**(1): E75-E84.
42. N. Oyama, H. Takahashi, M. Kawaguchi, et al., Effects of tissue pressure on transgene expression characteristics via renal local administration routes from ureter or renal artery in the rat kidney.

Pharmaceutics, 2020. **12**(2).

43. K. Nishimura, K. Ogawa, M. Kawaguchi, et al., Suppression of peritoneal fibrosis by sonoporation of hepatocyte growth factor gene-encoding plasmid DNA in mice. *Pharmaceutics*, 2021. **13**(1).
44. S. Fumoto, E. Kinoshita, K. Ohta, et al., A pH-adjustable tissue clearing solution that preserves lipid ultrastructures: suitable tissue clearing method for DDS evaluation. *Pharmaceutics*, 2020. **12**(11).
45. C.H. Fan, Y.H. Cheng, C.Y. Ting, et al., Ultrasound/magnetic targeting with SPIO-DOX-microbubble complex for image-guided drug delivery in brain tumors. *Theranostics*, 2016. **6**(10): 1542-56.